Magnetic and electronic properties of $La_{1-x}Sr_xCoO_3$ single crystals across the percolation metal-insulator transition

H. M. Aarbogh,[1] J. Wu,[1] L. Wang,[1] H. Zheng,[2] J. F. Mitchell,[2] and C. Leighton[1,*]
[1]*Department of Chemical Engineering and Materials Science, University of Minnesota, Minneapolis, Minnesota 55455, USA*
[2]*Materials Science Division, Argonne National Laboratory, Argonne, Illinois 60439, USA*
(Received 9 June 2006; published 12 October 2006)

Lightly doped $La_{1-x}Sr_xCoO_3$ single crystals (i.e., $x \leqslant 0.15$) have been intensively studied primarily due to the occurrence of spin-state transitions and magnetoelectronic phase separation. We report here the electronic transport and magnetic properties of more heavily doped crystals ($0.15 < x < 0.30$) with compositions clustered around the percolation metal-insulator transition (MIT). While the magnetic ordering temperature and saturation magnetization increase gradually as x is increased above 0.17, the resistivity and coercivity show drastic decreases in the range $0.17 < x < 0.20$, due to the percolation and coalescence of the metallic ferromagnetic (FM) clusters that form in a semiconducting non-FM matrix at low doping. The doping dependence of the coercivity can be qualitatively understood in terms of the thermal stability of isolated FM clusters and the formation of domains in percolated networks. The magnetoresistance shows a smooth crossover from the intergranular giant magnetoresistance (GMR)-type behavior that is dominant at low x (due to spin-dependent transport between FM clusters) to the conventional negative magnetoresistance occurring in the vicinity of the ordering temperature at high x. These two mechanisms coexist in the range $0.17 < x < 0.20$, providing further evidence of the spatial coexistence of insulating and metallic phases. The data suggest that although magnetoelectronic phase separation certainly occurs, it may be active over a smaller doping range than in polycrystals. At a composition between $x=0.20$ and 0.30 the signatures of phase coexistence in the magnetotransport disappear. Interestingly, this is coincident with a transition in the high-temperature (above the Curie point) transport from semiconducting-like to metallic-like. The largest "colossal magnetoresistance-type" negative magnetoresistance effects on the metallic side of the MIT are ~20% in $La_{1-x}Sr_xCoO_3$, smaller than the equivalent manganites, due to the absence of close competition with a strongly insulating phase. The incompatibility of some of the relevant spin states and crystal symmetries with a static, coherent, Jahn-Teller distortion, and the absence of long-range antiferromagnetic order in the $La_{1-x}Sr_xCoO_3$ phase diagram are likely key factors in this regard.

DOI: 10.1103/PhysRevB.74.134408 PACS number(s): 75.47.Gk, 71.30+h, 72.15.Gd

I. INTRODUCTION

Although perovskite cobaltites have received less attention than their manganite counterparts, these materials are the subject of considerable recent interest.[1–29] This interest stems primarily from two important factors: (i) the cobaltites (e.g., $LaCoO_3$) display a subtle competition between intra-atomic Hund's-rule exchange (H_{ex}) and crystal-field splitting (Δ_{CF}) energies, meaning that an additional degree of freedom, the spin state of the Co ion,[1–15] is present in these materials and (ii) when (hole) doped with group II alkaline earth elements (e.g., by Sr in $La_{1-x}Sr_xCoO_3$) they exhibit a clear (and in some sense simple) form of magnetoelectronic phase separation.[16–25] The details of the spin-state behavior are controversial however, even in undoped $LaCoO_3$.[1–15] It is generally agreed upon that the low spin (LS) state ($t_{2g}^6 e_g^0$, $S=0$) is favored at $T=0$ due to the slight dominance of Δ_{CF} over H_{ex}, and that thermal excitation to a finite spin state occurs around 100 K. Controversy exists as to whether the resulting paramagnetism is due to an intermediate spin (IS, $t_{2g}^5 e_g^1$, $S=1$) or high spin (HS, $t_{2g}^4 e_g^2$, $S=2$) state, or a mixture of the two.[1–15] A second magnetic anomaly occurs at 500 K,[1–15] where the population of the various spin states appears to change once more, along with an apparent transition from semiconducting to metallic.[1–15,26–28] Sr doping adds a further layer of richness to the spin-state issue as a full description of the magnetic behavior requires assignment of a spin state to both Co^{3+} and Co^{4+} ions.

In addition to these spin-state phenomena, experimental techniques as widely varied as transmission electron microscopy,[18] nuclear magnetic resonance (NMR),[20–22] small-angle neutron scattering (SANS),[23] and neutron diffraction[18,25,29] have verified that magnetoelectronic phase separation occurs upon doping with Sr ions. Magnetoelectronic phase separation, where a system exhibits heterogeneity in electronic and magnetic properties even in the absence of chemical segregation, is a ubiquitous phenomenon in complex oxides. It has been observed in cuprates, manganites,[30,31] and cobaltites[16–25,29] and is correlated with some of their most prominent properties such as high-temperature superconductivity, colossal magnetoresistance (CMR), and multiferroic behavior. In the $La_{1-x}Sr_xCoO_3$ system the heterogeneity takes the form of ferromagnetic metallic (FMM) clusters that form in a non-FM semiconducting matrix at low doping.[16–25,29] As doping increases it is believed that the clusters coalesce at $x \approx 0.17$, leading to a percolation-type metal-insulator transition (MIT) to a metallic state and the coincident onset of long-range FM order.[16–25,29] Magnetic excitons have been found to form around oxygen defects in undoped $LaCoO_3$ (Ref. 32) and could well be the precursors to the nanoscopic FM-ordered clusters that eventually occur upon Sr doping.

Recently we have performed several investigations focused on establishing not only the phenomenology of the clustered state at low doping ($x<0.17$), but the consequences of the formation of this state for the electronic and magnetic properties of the materials.[20–24,33,34] Using a combination of ^{59}Co and ^{139}La NMR, SANS, magnetometry, and magnetotransport we established that (i) bulk polycrystalline specimens exhibit spatial coexistence of multiple magnetic phases at all doping levels;[20–22] (ii) these phases compete in an unexpectedly complex manner as a function of doping, and particularly temperature;[22] (iii) approximately spherical FM clusters of size 20–30 Å form at low temperatures at $x=0.15$;[23] and (iv) long-range FM order exists at higher doping due to the coalescence of these clusters.[20–24,33,34] In terms of the consequences of this phase separation for the physical properties of the materials, it was established that the formation of these FMM clusters in a non-FM semiconducting matrix provides a naturally occurring analog to the artificial systems fabricated by depositing nanometer-scale FM metallic particles in insulating matrices such as Co-SiO_2, i.e., the system exhibits an intergranular giant magnetoresistance (GMR) effect due to spin-dependent transport between isolated clusters.[23] Single-crystal specimens also exhibit glassy transport effects,[34] which are reminiscent of some of the phenomena observed in the relaxor ferroelectrics, which are known to form a phase-separated state of nanoscopic ferroelectric clusters embedded in a nonferroelectric matrix. In summary, it is clear that at low doping ($x<0.17$) a clustered state is formed and that it has profound consequences for the magnetoelectronic properties of the material.

In this paper we focus on the composition range near to, and just above, the critical composition ($x_C \approx 0.17$) where the cluster coalescence leads to a percolation transition to a metallic state and the coincident onset of long-range FM order. We probe this regime using multiple single-crystal samples with compositions clustered in the range $0.17<x<0.30$. It is worth noting that this regime has been less intensively studied, particularly in single crystals, as the synthesis of high-quality oxygen stoichiometric crystals becomes increasingly difficult at higher doping. Single-crystal samples allow us to probe truly intrinsic transport and coercive properties, two of the most important aspects of this work. Magnetometry, electronic transport, and magnetotransport measurements reveal a steady increase in saturation magnetization and magnetic ordering temperature with increasing doping, consistent with the prior measurements on polycrystalline samples.[33] The resistivity and coercivity however, show a rapid decrease across a very small composition range between $x=0.17$ and 0.20, both being due to the coalescence of FMM clusters into a long-range-ordered metallic FM network. Magnetoresistance measurements show a smooth crossover from the aforementioned intergranular GMR effect[23] at low doping, to a more conventional negative MR for higher doping. The intergranular GMR is associated with transport between isolated clusters and is dominant at $x=0.15$ (i.e., below the critical composition), while the negative MR occurring at high doping (in the metallic state) occurs near the Curie temperature, similar to the CMR seen in manganites.[30,31,35,36] The observation of coexistence of these two forms of MR is taken as further evidence for magnetoelectronic phase separation, perhaps over a smaller doping range than seen in polycrystals. For the case of $La_{1-x}Sr_xCoO_3$ the "CMR-type" negative MR is of order 20%, smaller than the manganites.[30,31,35,36] We interpret this in terms of the absence of close competition with a strongly insulating phase such as a Jahn-Teller polaron state or a charge- and orbitally-ordered antiferromagnetic (AF) insulating phase, as occurs in many manganite systems[30,31,35,36] and is correlated with the largest CMR effects.[37] The rhombohedral crystal symmetry (space group $R\bar{3}c$) of $La_{1-x}Sr_xCoO_3$ ($x<0.30$) (see, for example, Refs. 16–18) being incompatible with a static, coherent, Jahn-Teller distortion, the fact that only some of the possible Co ion spin states are Jahn-Teller active, and the absence of a long-range ordered AF phase in the $La_{1-x}Sr_xCoO_3$ phase diagram (see, for example, Refs. 18 and 33) are all important in this regard.

II. EXPERIMENTAL CONSIDERATIONS

The single-crystal samples used in this study were taken from the same series of samples described in prior work.[23,34] We studied samples with doping of $x=0.15$, 0.17, 0.18, 0.19, 0.20, and 0.30, i.e., focused near to, and on the metallic side of, the MIT. The crystals were grown by the floating zone method in an NEC SC-15HD infrared mirror furnace at Argonne National Laboratory. They were proven single crystal and single phase by x-ray and neutron diffraction and were further characterized by energy-dispersive spectroscopy, thermogravimetric analysis, and measurement of sample mass before and after oxygen annealing treatments. dc magnetization measurements were performed in a commercial Quantum Design system using the extraction method, from 5 to 300 K in magnetic fields up to 40 kOe. Electronic-transport measurements were made using an ac resistance bridge operating at 13.7 Hz in a four-wire van der Pauw geometry from 5 to 300 K in fields up to 90 kOe. Indium contacts were employed and were Ohmic down to the lowest temperature measured. All measurements were made with the magnetic field aligned along the [111] direction (using pseudocubic notation). For transport measurements the injected current was perpendicular to this field.

III. RESULTS AND DISCUSSION

A. Magnetic properties

The temperature dependence of the dc magnetization (M) is shown in Fig. 1 for $x=0.17$, 0.18, 0.19, 0.20, and 0.30 after field cooling in 100 Oe. The two curves shown in each case are for measuring fields (H) of 100 and 10 kOe. Starting at $x=0.30$ we observe FM behavior with a Curie temperature (T_C) of approximately 225 K as estimated from the $M(T)$ curve for $H=100$ Oe, i.e., low field. This is in close agreement with prior work on polycrystals,[33] which indicated $T_C \approx 225$ K at this composition. In the higher measuring field of 10 kOe the FM to paramagnet transition is broadened and appears shifted to higher T, as is normally the case. As x decreases from 0.20 to 0.18, T_C exhibits a weak decrease from about 175 K down to 165 K [again estimated from the low field $M(T)$], the low-T magnetization shows a similar

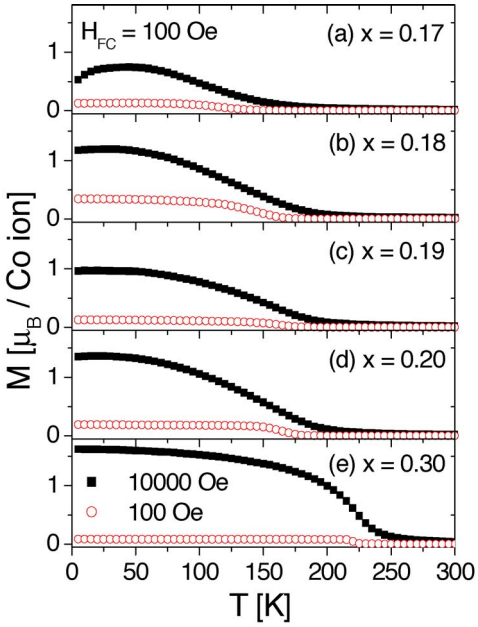

FIG. 1. (Color online) Temperature dependence of the magnetization of $x=0.17$ (a), 0.18 (b), 0.19 (c), 0.20 (d), and 0.30 (e) single crystals measured in 100 Oe (open points) and 10 kOe (closed points) magnetic fields. The samples were cooled in a 100 Oe field.

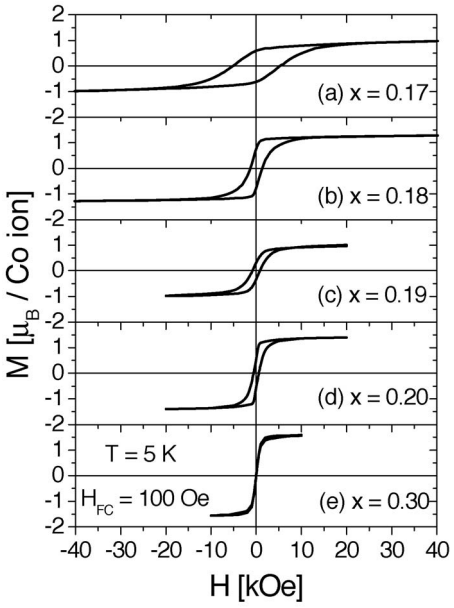

FIG. 2. Magnetization hysteresis loops of x=0.17 (a), 0.18 (b), 0.19 (c), 0.20 (d), and 0.30 (e) single crystals measured at 5 K after field cooling in 100 Oe.

small decrease, while the overall shape of $M(T)$ is barely altered. At $x=0.17$ however, the magnetic transition temperature has clearly undergone a significant decrease (to about 130 K), the high-field magnetization is distinctly reduced, and the $M(T)$ curve begins to take on an anomalous form. A great deal of prior work on low-doped single crystal and polycrystalline samples (e.g., Refs. 8, 17, 18, 22, 33, and 38–40) has shown that at $x<0.17$ the magnetic properties are best described by a spin—or cluster-glass state, which has been discussed in detail. A distinct freezing temperature is manifested as a peak in the zero-field-cooled (ZFC) $M(T)$ curve and a peak in the in-phase ac susceptibility, which shifts with frequency in a manner consistent with critical slowing down of the spin dynamics.[33] The field-cooled (FC) $M(T)$ curves exhibit a flattening near the freezing temperature in addition to bifurcation of ZFC and FC magnetizations.[33] These features have been observed in both polycrystalline and single-crystal samples. (See Ref. 34 for instance, for data on an $x=0.15$ single crystal). In summary, the data at $x=0.17$ begin to show a crossover from the FM state that is clearly dominant at $x=0.30$, to the glassy state that is dominant at $x=0.15$. This composition is therefore very close to the critical composition separating the two regimes. Neutron diffraction[18,25,29] and SANS (Ref. 23) have been used to study this regime in single crystals and polycrystals and show a clear evolution from short-range order due to the magnetism of the FM clusters to long-range FM order near $x=0.17$. NMR measurements on polycrystalline samples[22] further demonstrate that there appear to be three distinct magnetic phases at low doping. In addition to the FM phase in the clusters, the matrix was suggested to be composed of a spin- or cluster-glass phase in addition to a low-spin phase.

Corresponding $M(H)$ loops at $T=5$ K for the $x=0.17$, 0.18, 0.19, 0.20, and 0.30, compositions are shown in Fig. 2. These data were acquired by cooling in 100 Oe to 5 K then cycling the applied field through a complete loop, beginning at positive H. The data show that although the saturation magnetization (M_S) displays only a weak increase with increasing x, the remnance, saturation field, and coercivity (H_C) vary appreciably. Specifically, as x decreases from the FM state at $x=0.3$, H_C rapidly increases and the loops become increasingly sheared. At lower doping (it is particularly clear for $x=0.17$) there are indications of a nonsaturating component at high magnetic fields, as observed and commented on in polycrystals.[33] This is interpreted as the signature of the non-FM matrix, which becomes more dominant as x decreases, the long-range FM order is lost, and the non-FM phase fraction increases at the expense of the FM clusters. The evolution of M_S, T_C, and H_C with composition is shown more clearly in Fig. 3. The T_C values decrease more rapidly below $x=0.18$, consistent with the crossover from long-range-ordered FM to a clustered state, while M_S varies only weakly across the transition. [Note that Fig. 3(b) also includes the apparent "T_C" determined from resistivity and magnetoresistance, in addition to $M(T)$. These will be discussed later]. The rapid change in coercivity shown in Fig. 3 is noteworthy and is obviously related to the coalescence of isolated FM clusters into a long-range ordered network, which eventually dominates the magnetic response. We believe that the decrease in H_C is driven by the crossover from isolated FM particles, which are likely to be in a single-domain state, to a percolated network where domain formation occurs. The coercivity decreases as the clusters grow, and eventually percolate, due to magnetization reversal by domain-wall processes as opposed to rotation. This is similar to the general trend observed in small ferromagnetic particles;[41] at a fixed temperature, H_C first increases with

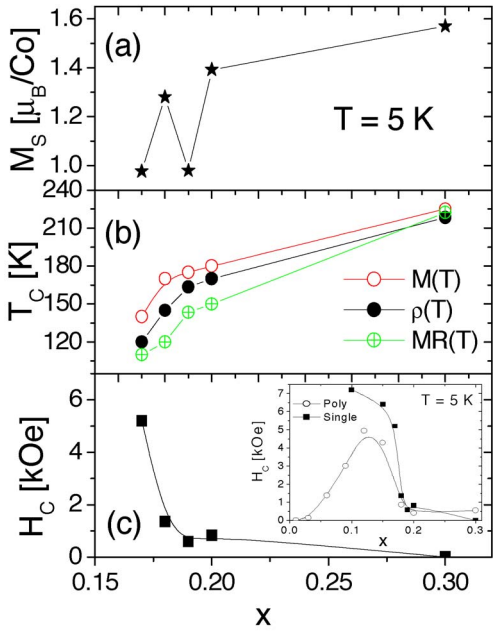

FIG. 3. (Color online) Sr doping dependence of (a) the 5 K saturation magnetization, (b) the magnetic transition temperature, and (c) the 5 K coercive field, of single-crystal samples with $0.17 < x < 0.30$. Inset to (c): Doping dependence of the 5 K coercive field of both polycrystalline and single-crystal samples over an expanded range from $x=0.0$ to 0.30. In (b) the transition temperatures measured from magnetometry, resistivity, and magnetoresistance are all shown. The solid lines are guides to the eye.

increasing particle diameter due to the transition from superparamagnetism to static order reflecting the increasing thermal stability. H_C then decreases above a certain diameter due to the transition from single-domain to multidomain states. Such a peak in H_C is indeed present in the polycrystalline samples we have investigated previously. The inset to Fig. 3(c) shows the 5 K coercivity of the single-crystal and polycrystal samples over an expanded doping scale ($0.01 < x < 0.30$). The polycrystalline samples clearly show the H_C peak, while the single crystals, which were grown with compositions clustered around the MIT, have dopings beyond the maximum in H_C. Studies of coercive behavior of small ferromagnetic particles embedded in nonmagnetic matrices[42] or initially isolated islands in thin ferromagnetic films[43,44] offer an even better analogy to the situation in $La_{1-x}Sr_xCoO_3$. Several studies have found similar decreases in coercivity as the percolation threshold is crossed,[42–44] which is typically explained in terms of the transition from isolated clusters (islands) to a long-range-ordered network with domain reversal.

The coercivity maximum occurring near $x=0.10$ in the inset in Fig. 3(c) suggests that the nanoscopic FM clusters are thermally stable at least for $x>0.10$, and possibly at even lower x. This is consistent with neutron diffraction data showing that indications of static FM ordering in nanoscopic clusters (the size of the regions can be calculated from the width of the diffraction peak) are already present at $x=0.10$.[18,25] At lower x values the situation is more complicated. Previous authors have emphasized the importance of blocking of superparmagnetic clusters for explaining the frequency and time-dependent magnetic properties,[17] while others have concluded that this behavior is due to a true spin or cluster-glass state,[33,28–40] which resides in the matrix.[22] In any case, given that the data of Fig. 3(c) suggest that the clusters are certainly thermally stable at $x=0.15$ (consistent with the observation of static FM order by neutron diffraction) we can make a simple estimate of the FM anisotropy required for this stability. At $x=0.15$ the neutron diffraction data of Phelan *et al.*[25] provide a cluster size of 15 Å (8 K), while the SANS data of our own suggests 15–25 Å at low T.[23] Equating $k_B T_B$, where T_B is the blocking temperature of the clusters, with $(4/3)\pi\xi^3 K$, where ξ is the cluster size and K is the anisotropy energy per unit volume, gives K values in the range 3×10^5 to 1×10^6 erg/cm^3 using a transition temperature of 125–150 K at $x=0.15$. These values are comparable to simple ferromagnets such as Co, demonstrating that physically reasonable values of anisotropy constants are consistent with the observed thermal stability of these nanoscopic clusters. To the best of our knowledge, the actual anisotropy constants of $La_{1-x}Sr_xCoO_3$ in the FM phase ($x>0.17$) have not been measured.

As a final comment on the coercivity data, we note that the H_C values obtained deep in the FM phase at $x=0.3$ (i.e., 10 Oe at 5 K) are significantly lower than those obtained on polycrystalline samples (e.g., 550 Oe at 35 K). This could be due to a significant density of domain-wall pinning sites in polycrystalline samples that is not present in single crystals. These pinning sites could simply be grain boundaries but it is also possible that domain walls are pinned by small clusters of residual non-FM phases that are present due to disorder in polycrystalline samples and absent in single crystals. It is important to point out that Co and La NMR measurements on polycrystals showed small fractions of residual non-FM phases even at high doping ($x>0.30$) (Refs. 20 and 22) consistent with the observation of nonsaturating components in $M(H)$ curves even at high x.[33] This is not the case for single-crystal samples [which show no nonsaturating component at $x>0.20$ (see Fig. 2)] and could indicate a narrower doping region over which phase separation is found in the less disordered single crystals. Further work comparing the NMR and magnetometry in polycrystals and single crystals will elucidate this point.

At this stage a comment on the implications of the M_S (x) data for the spin state of the Co ions is required. Attempting to determine uniquely the spin state of the two Co ions from magnetometry data is difficult and has been discussed in detail for polycrystalline samples.[33] It is particularly perilous to infer the likely spin state from saturation magnetization data taken from $M(H)$ loops (as opposed to high T Curie-Weiss behavior) as the existence of nonsaturating components to the magnetization significantly complicates the analysis. Regarding the current data it is sufficient to note that the values shown in Fig. 3 for these single crystals are rather close to those obtained in prior work on polycrystalline samples where it was suggested that the IS state for both Co^{3+} and Co^{4+} ions provides the best description of the data.[33] First-principles electronic-structure calculations show that hole doping enhances Co-O hybridization, stabilizing the interme-

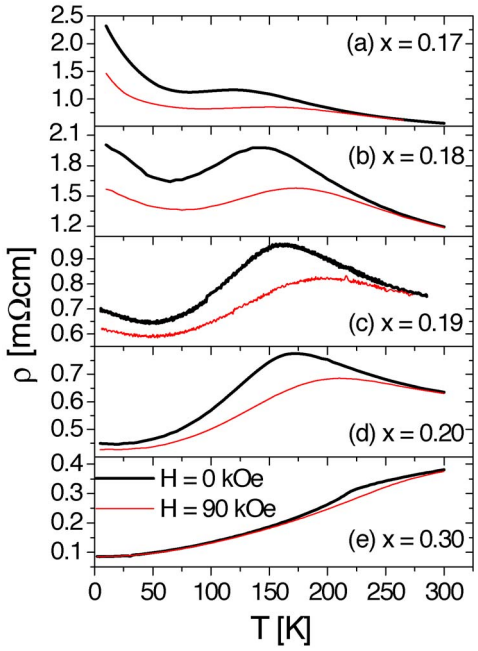

FIG. 4. (Color online) Temperature dependence of the resistivity of $x=0.17$ (a), 0.18 (b), 0.19 (c), 0.20 (d), and 0.30 (e) single crystals measured in zero field (heavy line) and 90 kOe (light line). The samples were zero-field cooled.

diate spin state and reducing the saturation magnetization compared to the simple ionic prediction.[45] Ravindran *et al.*[45] predict M_S values increasing from 1.57 to $1.67\mu_B$/Co between $x=0.2$ and 0.3, comparing reasonably well to our values of 1.4 and $1.55\mu_B$/Co, respectively. Values of the effective number of Bohr magnetons from fits to the high-temperature Curie-Weiss behavior are also consistent with the IS state for both ions.

B. Transport and magnetotransport properties

We turn now to the electronic properties of the $La_{1-x}Sr_xCoO_3$ crystals. Figure 4 shows the temperature dependence of the electrical resistivity (ρ) for $x=0.17$, 0.18, 0.19, 0.20, and 0.30 measured in $H=0$ and 90 kOe. Examining first the zero-magnetic-field data, it can be seen that at $x=0.17$ a semiconducting-like behavior is apparent at low T ($d\rho/dT<0$), while a metallic-like temperature dependence ($d\rho/dT>0$) is active for $x=0.3$. Prior measurements of the low-temperature conductivity[34] for $0.0<x<0.20$ have shown that a finite $T=0$ extrapolation of the conductivity first occurs at $x=0.17$, demonstrating that all of the samples shown in Fig. 4 (i.e., $0.17<x<0.30$) are in fact on the metallic side of the percolation MIT, which occurs between $x=0.15$ and 0.17 in single crystals. As discussed in more detail below, these transport data, in particular the magnetoresistance (MR), provide strong evidence of an inhomogeneous MIT, i.e., a percolation transition where a metallic path threads an insulating matrix leading to inhomogeneous current flow. Regarding the influence of magnetic ordering on resistivity, the inflection point near T_C at $x=0.30$, evolves into a peak in $\rho(T)$ at T_C for $x=0.20$, 0.19, 0.18, and 0.17, reflecting the fact that, at $T>T_C$, a transition from a metallic-like temperature dependence to an insulating-like temperature dependence occurs between $x=0.30$ and 0.20. A similar feature was observed in the polycrystalline phase diagram near $x=0.30$. Note that the peak in $\rho(T)$ actually occurs at a temperature just below (by 10 to 20 K) the T_C determined from $M(T)$, as shown in Fig. 3(b). Resistivity peaks occurring at temperatures slightly lower than the apparent T_C from magnetometry is the usual case in the manganites.[30,31,35,36] At $x=0.17$ the feature at T_C is very weak and broad, and at $x=0.15$ (see prior work) it vanishes completely. These observations are consistent with the phase separation/percolation MIT scenario already discussed in the previous section on magnetic properties; for $x\leqslant 0.15$ no percolative (FMM) current path through the non-FM semiconducting regions is present, meaning that no feature is observed in $\rho(T)$ near T_C. On the other hand, for $x>0.17$ the majority of the excitation current flows through the percolated metallic path meaning that the peak in $\rho(T)$ near the ordering temperature is evident. In this region the onset of a metallic behavior on cooling through T_C is interpreted as being due to the double-exchange interaction between Co ions with differing valence, which simultaneously favors delocalization and FM ordering.

Examining the results obtained in a large applied field (90 kOe) we observe a distinct crossover in behavior from $x=0.30$ to 0.17. At $x=0.30$ the only MR contribution appears to occur in the vicinity of T_C, where a negative MR is observed. As x decreases a second MR contribution is observed, again negative, this time occurring only at the lowest T. At $x=0.17$ the low T contribution becomes the dominant form of MR and by $x=0.15$ the contribution near T_c has disappeared all together. The 90 kOe MR extracted from the zero-field and high-field curves of Fig. 4 is displayed in Fig. 5 for each of the samples studied. The crossover from a negative MR occurring only in the vicinity of T_C in the purely metallic phase, to a low-T negative MR occurring in the semiconducting phase is apparent. We believe that these data are again consistent with the phase separation/percolation MIT scenario. The negative MR near T_C clearly occurs due to current flow through the FMM percolative path while the low-T MR associated with the semiconducting phase, where the clusters are isolated, is due to the intergranular GMR effect we previously reported.[23] The latter mechanism involves spin-dependent transport between FMM clusters. The field dependence is quantitatively consistent with this mechanism (increased alignment of neighboring clusters by the applied field leads to increases in the transport probability, and therefore the conductivity, which scales with the square of the reduced magnetization[46,47]), as is the temperature dependence (the Coulomb energy penalty associated with individual electron-charging events leads to a distinctive form of hopping conduction[48–50]). Importantly, it is clear from Figs. 4 and 5 that both MR mechanisms are active for samples with $x=0.17$, 0.18, and 0.19. This directly implies that at these compositions the phase separation results in a situation where the system is barely percolated and the transport current flows both through insulating and metallic regions. It is important to point out that although these data are

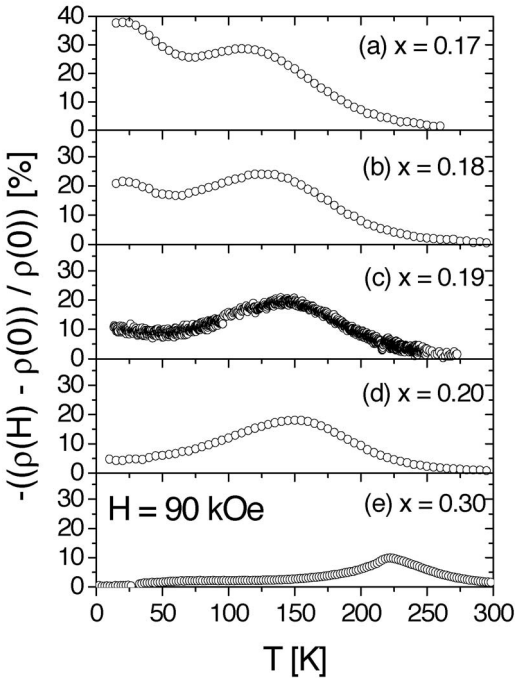

FIG. 5. Temperature dependence of the magnetoresistance $\{[\rho(H)-\rho(0)]/\rho(0)\}$ of $x=0.17$ (a), 0.18 (b), 0.19 (c), 0.20 (d), and 0.30 (e) single crystals measured in 90 kOe. These data were extracted from the data of Fig. 4.

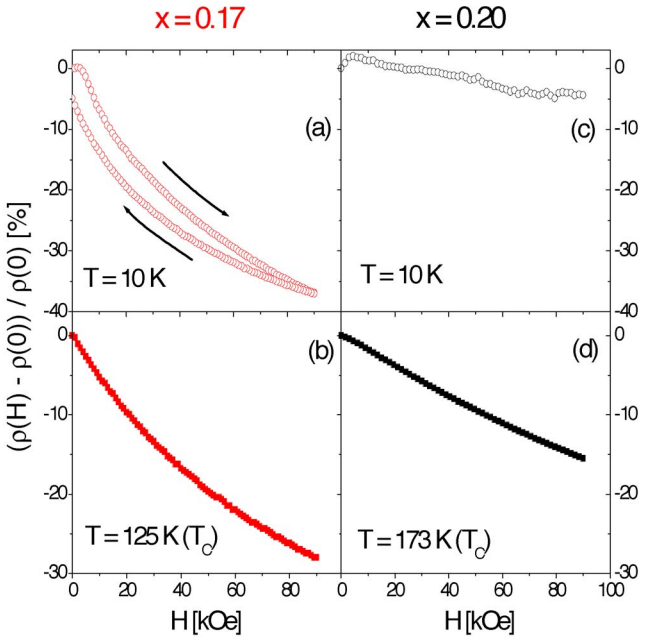

FIG. 6. (Color online) Magnetic-field dependence of the magnetoresistance $\{[\rho(H)-\rho(0)]/\rho(0)\}$ of $x=0.17$ [left panel, (a) and (b)] and $x=0.20$ [right panel, (c) and (d)] single crystals measured at $T=10$ K (top) and $T=T_C$ (bottom). The T_C in each case is noted on the figure.

consistent with a phase inhomogeneity picture, it is not clear from these data alone whether this is a result of a truly intrinsic electronic-phase separation in the absence of any chemical inhomogeneities (e.g., in doping or oxygen stoichiometry), or whether a small but significant chemical inhomogeneity is responsible. Comparing to the polycrystalline case we see that the region over which the phase separation occurs would appear to be somewhat smaller in single crystals, as implied by the magnetization data discussed above. For polycrystals the low-T MR persists well into the metallic phase (beyond $x=0.30$),[33] whereas in the single crystals it disappears certainly by $x=0.30$ and possibly as quickly as $x=0.20$. This comparison must be treated with some caution as the well-known effect of spin-dependent tunneling between polycrystalline grains through an insulating grain boundary[36] also leads to a negative MR at low T, which could mimic a GMR-type effect due to transport between FMM clusters, complicating our comparison. Having said this, we would like to point out an intriguing correlation between the doping level at which the phase separation ends and the system seems to enter a homogeneous FMM state, and the high-T transport behavior. Specifically, we can see from Fig. 7(b) and Figs. 4(d) and 4(e) that the doping level at which the low-T MR disappears is identical to that at which the sign change in $d\rho/dT$ occurs for $T>T_C$. Such a correlation between the nature of the high-T transport and the eventual vanishing of the phase-separated state has in fact been envisioned.[51]

Further proof of the validity of our decomposition of the MR into these two distinct mechanisms associated with the semiconducting and metallic phases is provided by the field-dependent data of Fig. 6. This figure displays the magnetic-field dependence of the MR ratio for $x=0.17$ and 0.20 samples at both low T (10 K) and near T_C (125 and 173 K, respectively). The data were collected by cooling to the measurement temperature in $H=0$ then sweeping from $H=0$ to 90 kOe. In the cases where hysteresis is observed the data are also shown for sweeping back from 90 kOe to 0. The behavior at these two compositions is dramatically different, highlighting the rapid evolution in magnetotransport properties across the percolation MIT. At $x=0.20$ the low-T MR is small ($<5\%$ in 90 kOe), while the dominant MR occurs near T_C. At $x=0.17$ a similar form of MR(H) is observed near the magnetic-transition temperature, but a distinctly different form occurs at low T. The low-T MR shows the characteristic hysteresis of the intergranular GMR-type effect we previously reported (continuing the field sweep to negative fields results in a peak in $\rho(H)$ at H_C),[23] in addition to differences between the virgin curve and subsequent field sweeps. Again, the clear observation of both of the active MR mechanisms in the $x=0.17$ case [see Figs. 6(a) and 6(b)] is strong evidence for current flow through both semiconducting (non-FM) and barely percolated metallic (FM) regions, i.e., a spatially inhomogeneous percolation MIT.

The transport and magnetotransport data are summarized in Fig. 7, which plots the zero-field resistivity, $T=15$ K MR, and $T=T_C$ MR, as a function of doping. These data illustrate (i) the rapid reduction in resistivity at the percolation transition, (ii) the reduction in low-T MR with increasing doping due to the decrease in non-FM phase fraction and the dominance of the FMM phase, and (iii) the vanishing of the MR near T_C when the semiconducting phase is entered and a FMM path no longer percolates through the system.

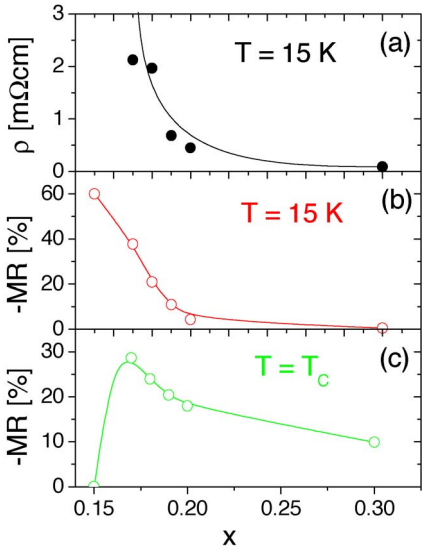

FIG. 7. (Color online) Sr doping dependence of (a) the 15 K zero-field resistivity, (b) the 15 K magnetoresistance, and (c) the magnetoresistance at T_C, of single-crystal samples with $0.15<x<0.30$. Note that in both cases the magnetoresistance values are negative. The solid lines are guides to the eye.

The specific form and magnitude of the variation in the MR at T_C with doping is worthy of further comment. First, the MR ratios vary between 10% and 28% between $x=0.30$ and 0.17, significantly smaller than that seen in comparable manganites. For instance, single-crystal $La_{1-x}Sr_xMnO_3$ at $x=0.18$ exhibits MR ratios (using the same definition that we adopt in this paper, i.e., $MR=[\rho(H)-\rho(H=0)]/\rho(H=0)$ of over 75% in 80 kOe.[35] Similar values are found in the FM phase of $La_{1-x}Ca_xMnO_3$.[30,31,35,36] It is now understood, from the vast body of knowledge acquired on the manganite systems[30,31,35,36] and the eventual compilation of the global-phase diagram,[37] that the CMR values are maximized in the regions of the phase space where a FMM state is in close and direct competition with a strongly insulating phase. Systems such as $Pr_{1-x}(Ca,Sr)_xMnO_3$, where the tolerance factor (and hence one-electron bandwidth) can be varied while keeping the doping constant, illustrate this point very well as they can achieve $\rho(H)/\rho(H=0)$ of 10^{11} in applied fields of only 20 kOe.[52,53] This colossal response is attained when the phase competition between FMM and insulating phases is maximized. The competing insulating state can exhibit charge or orbital ordering (or both),[30,31,35,36] long-range AF order,[30,31,35,36] or charge localization due to the formation of Jahn-Teller polarons.[30,31,35,36,54,55] We believe that the smaller CMR effect observed in the cobaltites is due to the fact that the ingredients required for the existence of this strongly insulating state are not present. First, there is no long-range-ordered AF phase in the entire $La_{1-x}Sr_xCoO_3$ phase diagram.[17,33] The end members are a diamagnetic (at least at $T=0$, see above for a discussion of spin-state transition issues) semiconductor ($x=0$) and a ferromagnetic metal ($x=1$),[56] and no AF phase has been reported at any intermediate composition. Note that AF interactions (i.e., a negative Curie-Weiss temperature) have been observed in the finite spin states of $LaCoO_3$, as have AF fluctuations in neutron-scattering experiments,[8,25,57] but no static AF ordering is known to occur. Second, it is important to point out that the crystal symmetry of $La_{1-x}Sr_xCoO_3$, at least for $x<0.3-0.5$, is rhombohedral (space group $R\bar{3}c$),[18] meaning that a coherent, static, Jahn-Teller distortion is disallowed.[58] The localization of charge carriers via the formation of Jahn-Teller polarons is therefore less effective than in many manganites. Note that the work of Louca *et al.*[59] has shown that although a static and coherent Jahn-Teller distortion is not possible in the doping range of interest here, dynamic Jahn-Teller distortions can be observed by neutron scattering. These distortions could play some role in electron localization. The final point to be made regarding the difficulties with achieving effective localization due to Jahn-Teller polaron formation is that only the IS state of the Co^{3+} and Co^{4+} ions is Jahn-Teller active. In fact, Phelan *et al.*[25] have nicely demonstrated the onset of dynamical orbital ordering in $LaCoO_3$ due to the thermally driven transition from LS to IS states. In addition, to the best of our knowledge there have been no reports of charge ordering in $La_{1-x}Sr_xCoO_3$. It is clear from the above arguments that there are several factors that contribute to the absence of a strongly insulating state in $La_{1-x}Sr_xCoO_3$. With no such state present to compete with the FMM phase, the MR values achieved near T_C are modest. Note though that the MR near T_C does actually increase with decreasing doping (in the metallic phase) reaching a maximum very close to the MIT. This is consistent with the general argument that the MR should increase when phase competition is present, i.e., a small enhancement in MR occurs as the phase boundary between FMM and weakly semiconducting non-FM is approached.

At high doping, deep in the metallic phase (i.e., $x=0.3$), it is noteworthy that the MR is quite small (10%) and that it shows a sharp peak very close to T_C [see Fig. 5(e)]. Examination of Fig. 3(b) reveals that at this composition the T_c determined from $M(T)$, the peak in the zero field $\rho(T)$, and the MR peak are essentially coincident. We concur with Yeh *et al.*[60] that conventional spin-disorder scattering near the transition from paramagnet to double-exchange FM is the likely mechanism for the MR in this situation. Note also that the reduction in resistivity from $T=T_C$ to $T=0$ is of order 2–3 in the metallic crystals, reasonably consistent with double exchange alone. This suggests that polaronic conduction and electron-correlation effects may be less important than in manganites. The fact that the MR and resistivity-peak temperatures fall well below the actual T_C at lower doping values [where the MIT is approached, see Fig. 7(c)] is consistent with the increased MR values and can be ascribed to the aforementioned competition between FMM and non-FM semiconducting phases.

As a final remark on the magnetotransport data we would like to make a comparison between the MR mechanisms we believe are at play here and others that have been advanced to describe phase-separated systems. Many prior works on phase separation have described a mechanism where the large MR effects occur due to an increase in the volume of the FM regions with magnetic field, leading to a field-driven percolation transition. We do not believe that such a field-

driven growth of FMM clusters is responsible for the MR we observe here for the following reasons; (i) Various neutron-scattering studies[18,19,23,25,29] have found that the phase separation occurs only on nanoscopic rather than microscopic length scales; (ii) the data shown in this paper and prior work at $x=0.15$ show conclusively that even for dopings very close to the percolation MIT it is not possible to drive a transition from insulating to metallic with the application of fields up to 90 kOe; (iii) the MR we observe in the insulating phase is consistent, both qualitatively and quantitatively, with spin-dependent transport between isolated clusters, i.e., it relies on the alignment of neighboring clusters rather than field-driven expansion; (iv) no metamagnetic-type $M(H)$ behavior is observed where the magnetization undergoes rapid increases at a certain value of H due to increases in volume fraction of the FM phase at the expense of the non-FM phase; (v) the NMR measurements on this system (which necessarily involve the application of large magnetic fields) show that phase coexistence is observed even out to large H, meaning that the FM regions do not overwhelm the matrix at high field; and finally, (vi) preliminary high-field SANS data do not reveal a marked increase in cluster size with increasing field. Further high-field work with neutron scattering will hopefully clarify this issue further. It is possible that a weak increase occurs with increasing field, but not to the point of a field-induced percolation. Although the field-driven cluster growth picture does not seem to apply to $La_{1-x}Sr_xCoO_3$ it does work well for some manganite systems. We hope that future work will address the possibility that this is related to the issue of nanoscopic versus microscopic phase separation in magnetic oxides. The $La_{1-x}Sr_xCoO_3$ system apparently exhibits phase coexistence on nanoscopic length scales and does not show a field-driven growth of FMM clusters, whereas other manganite systems display the phase segregation on much larger length scales and *do* show field-induced growth of the FM phase.

IV. SUMMARY AND CONCLUSIONS

We have presented the electronic and magnetic properties (with particular emphasis on coercivity and magnetoresistance) of $La_{1-x}Sr_xCoO_3$ single crystals with dopings clustered near the metal-insulator transition. The percolation transition has a strong influence on the coercive mechanisms, which can be understood in terms of thermal stability and domain formation issues. The thermal stability of the clusters at relatively low doping, along with previously determined cluster sizes, permit an estimate of the anisotropy required to support this thermal stability, which is of reasonable magnitude. Two distinct magnetoresistance contributions are observed, one associated with spin-dependent transport between ferromagnetic clusters in the semiconducting phase, the other associated with field-induced suppression of spin-disorder scattering. Importantly, these two mechanisms are observed to coexist up to $x=0.20$, consistent with magneto-electronic phase coexistence, although the doping range over which phase separation is implied is smaller than that seen in polycrystals. We have noted that the point at which the system seems to enter a homogeneous ferromagnetic metallic phase coincides with a crossover from an insulating-like to metallic-like temperature dependence of the resistivity at high temperatures. The magnetoresistance in the ferromagnetic metallic phase is found to be smaller than that seen in equivalent manganites, which is ascribed to the absence of competition with a strongly insulating phase. Finally, we have remarked that the generally accepted picture of large magnetoresistance occurring due to field-induced expansion of ferromagnetic regions (and their eventual percolation) may not be applicable to these cobaltites, which display phase segregation only on a nanoscopic scale.

ACKNOWLEDGMENTS

This work was supported by the DOE through Grant No. DE-FG02-06ER46275, NSF through Grant No. 0509666, and the donors of the ACS PRF. We would like to acknowledge fruitful discussions with W. Moulton, M. Hoch, I. Terry, and V. Dobrosavljevic.

*Corresponding author. Email address: leighton@umn.edu

[1] M. Imada, A. Fujimori, and Y. Tokura, Rev. Mod. Phys. **70**, 1039 (1998).
[2] K. Asai, O. Yokokura, N. Nishimori, H. Chou, J. M. Tranquada, G. Shirane, S. Higuchi, Y. Okajima, and K. Kohn, Phys. Rev. B **50**, 3025 (1994).
[3] M. A. Korotin, S. Yu. Ezhov, I. V. Solovyey, V. I. Anisimov, D. I. Khomskii, and G. A. Sawatzky, Phys. Rev. B **54**, 5309 (1996).
[4] S. Yamaguchi, Y. Okimoto, and Y. Tokura, Phys. Rev. B **55**, R8666 (1997).
[5] Y. Kobayashi, N. Fujiwara, S. Murata, K. Asai, and H. Yasuoka, Phys. Rev. B **62**, 410 (2000).
[6] S. Yamaguchi, Y. Okimoto, H. Taniguchi, and Y. Tokura, Phys. Rev. B **53**, R2926 (1996).
[7] C. Zobel, M. Kriener, D. Bruns, J. Baier, M. Gruninger, T. Lorenz, P. Reuter, and R. Revolevschi, Phys. Rev. B **66**, 020402 (2002).
[8] K. Asai, P. Gehring, H. Chou, and G. Shirane, Phys. Rev. B **40**, 10982 (1989).
[9] M. Itoh, M. Sugahara, I. Natori, and K. Motoya, J. Phys. Soc. Jpn. **64**, 3967 (1995).
[10] T. Kyomen, Y. Asaka, and M. Itoh, Phys. Rev. B **71**, 024418 (2005).
[11] K. Tsutsui, J. Inoue, and S. Maekawa, Phys. Rev. B **59**, 4549 (1999).
[12] S. Noguchi, S. Kawamata, K. Okuda, H. Nojiri, and M. Motokawa, Phys. Rev. B **66**, 094404 (2002).
[13] P. G. Radaelli and S.-W. Cheong, Phys. Rev. B **66**, 094408 (2002).
[14] K. Asai, A. Yoneda, O. Yokokura, J. M. Tranquada, G. Shirane, and K. Kohn, J. Phys. Soc. Jpn. **67**, 290 (1998).

[15] G. Maris, Y. Ren, V. Volotchaev, C. Zobel, T. Lorenz, and T. T. M. Palstra, Phys. Rev. B **67**, 224423 (2003).
[16] P. M. Raccah and J. B. Goodenough, J. Appl. Phys. **39**, 1209 (1968).
[17] M. A. Senaris-Rodriguez and J. B. Goodenough, J. Solid State Chem. **118**, 323 (1995).
[18] R. Caciuffo, D. Rinaldi, G. Barucca, J. Mira, J. Rivas, M. A. Senaris-Rodriguez, P. G. Radaelli, D. Fiorani, and J. B. Goodenough, Phys. Rev. B **59**, 1068 (1999).
[19] R. Caciuffo, J. Mira, J. Rivas, M. A. Senaris-Rodriguez, P. G. Radaelli, F. Carsughi, D. Fiorani, and J. B. Goodenough, Europhys. Lett. **45**, 399 (1999).
[20] P. L. Kuhns, M. J. R. Hoch, W. G. Moulton, A. P. Reyes, J. Wu, and C. Leighton, Phys. Rev. Lett. **91**, 127202 (2003).
[21] M. J. R. Hoch, P. L. Kuhns, W. G. Moulton, A. P. Reyes, J. Wu, and C. Leighton, Phys. Rev. B **69**, 014425 (2004).
[22] M. J. R. Hoch, P. L. Kuhns, W. G. Moulton, A. P. Reyes, J. Wu, and C. Leighton, Phys. Rev. B **70**, 174443 (2004).
[23] J. Wu, J. W. Lynn, C. J. Glinka, J. Burley, H. Zheng, J. F. Mitchell, and C. Leighton, Phys. Rev. Lett. **94**, 037201 (2005).
[24] J. E. Davies, J. Wu, C. Leighton, and K. Liu, Phys. Rev. B **72**, 134419 (2005).
[25] D. Phelan, D. Louca, S. Rosenkranz, S.-H. Lee, Y. Qiu, P. J. Chupas, R. Osborn, H. Zheng, J. F. Mitchell, J. R. D. Copley, J. L. Sarrao, and Y. Moritomo, Phys. Rev. Lett. **96**, 027201 (2006).
[26] R. R. Heikes, R. C. Miller, and R. Mazelsky, Physica (Amsterdam) **30**, 1600 (1964).
[27] S. Yamaguchi, Y. Okimoto, and Y. Tokura, Phys. Rev. B **54**, R11022 (1996).
[28] S. R. English, J. Wu, and C. Leighton, Phys. Rev. B **65**, 220407(R) (2002).
[29] V. V. Sikolenko, A. P. Sazonov, I. O. Troyanchuk, D. Tobbens, U. Zimmermann, E. V. Pomjakushina, and H. Szymczak, J. Phys.: Condens. Matter **16**, 7313 (2004).
[30] E. Dagotto, *Nanoscale Phase Separation and Colossal Magnetoresistance* (Springer, New York, 2002).
[31] E. Dagotto, T. Hotta, and A. Moreo, Phys. Rep. **344**, 1 (2001).
[32] S. R. Giblin, I. Terry, S. Clarke, T. Prokscha, A. T. Boothroyd, J. Wu, and C. Leighton, Europhys. Lett. **70**, 677 (2005).
[33] J. Wu and C. Leighton, Phys. Rev. B **67**, 174408 (2003).
[34] J. Wu, H. Zheng, J. F. Mitchell, and C. Leighton, Phys. Rev. B **73**, 020404(R) (2006).
[35] Y. Tokura and Y. Tomioka, J. Magn. Magn. Mater. **200**, 1 (1999).
[36] J. M. D. Coey, M. Viret, and S. von Molnár, Adv. Phys. **48**, 167 (1999).
[37] Y. Tomioka and Y. Tokura, Phys. Rev. B **70**, 014432 (2004).
[38] D. N. H. Nam, K. Jonason, P. Nordblad, N. V. Khiem, and N. X. Phuc, Phys. Rev. B **59**, 4189 (1999).
[39] D. N. H. Nam, R. Mathieu, P. Nordblad, N. V. Khiem, and N. X. Phuc, Phys. Rev. B **62**, 8989 (2000).
[40] S. Mukherjee, R. Ranganathan, P. S. Anilkumar, and P. A. Joy, Phys. Rev. B **54**, 9267 (1996).
[41] B. D. Cullity, in *Introduction to Magnetic Materials*, edited by M. Cohen, Addison-Wesley Series in Metallurgy and Materials (Addison-Wesley, Reading, MA, 1972).
[42] G. Xiao and C. L. Chien, Appl. Phys. Lett. **51**, 1280 (1987).
[43] J. M. Choi, S. Kim, I. K. Schuller, S. M. Paik, and C. N. Whang, J. Magn. Magn. Mater. **191**, 54 (1999).
[44] J. M. Lopez, R. Ramirez, M. Kiwi, M. J. Pechan, J. Z. Hill, S. Kim, H. Suhl, and I. K. Schuller, Phys. Rev. B **63**, 060401 (2000).
[45] P. Ravindran, H. Fjellvag, A. Kjekshus, P. Blaha, K. Scwarz, and J. Luitz, J. Appl. Phys. **91**, 291 (2002).
[46] J. Q. Xiao, J. S. Jiang, and C. L. Chien, Phys. Rev. Lett. **68**, 3749 (1992).
[47] S. Barzilai, Y. Goldstein, I. Balberg, and J. S. Helman, Phys. Rev. B **23**, 1809 (1981).
[48] P. Sheng, B. Abeles, and Y. Arie, Phys. Rev. Lett. **31**, 44 (1973).
[49] M. Pollak and C. J. Adkins, Philos. Mag. B **65**, 855 (1992).
[50] J. Zhang and B. I. Shklovskii, Phys. Rev. B **70**, 115317 (2004).
[51] V. Dobrosavljevic (private communication).
[52] J. Wu, H. Zheng, J. F. Mitchell, and C. Leighton, J. Magn. Magn. Mater. **288**, 146 (2004).
[53] Y. Tomioka and Y. Tokura, Phys. Rev. B **66**, 104416 (2002).
[54] C. P. Adams, J. W. Lynn, Y. M. Mukovskii, A. A. Arsenov, and D. A. Shulyatev, Phys. Rev. Lett. **85**, 3954 (2000).
[55] N. Mannela, A. Rosenbahn, C. H. Booth, S. Marchesini, B. S. Mun, S.-H. Yang, K. Ibrahim, Y. Tomioka, and C. S. Fadley, Phys. Rev. Lett. **92**, 166401 (2004).
[56] S. Kawasaki, M. Takano, and Y. Takeda,J. Solid State Chem. **121**, 174 (1996).
[57] Y. Kobayashi, S. Murata, K. Asai, J. M. Tranquada, G. Shirane, and K. Kohn, J. Phys. Soc. Jpn. **68**, 1011 (1999).
[58] A lowering of symmetry to monoclinic has been claimed for $LaCoO_3$ and would be consistent with a coherent Jahn-Teller distortion and orbital ordering, Ref. 15.
[59] D. Louca and J. L. Sarrao, Phys. Rev. Lett. **91**, 155501 (2003).
[60] N.-C. Yeh, R. P. Vasquez, D. A. Beam, C.-C. Fu, J. Huynh, and G. Beach, J. Phys.: Condens. Matter **9**, 3713 (1997).